

Automatic channel detection using deep learning

Nam Pham¹, Sergey Fomel¹, and Dallas Dunlap¹

Abstract

We have developed a method based on an encoder-decoder convolutional neural network for automatic channel detection in 3D seismic volumes. We use two architectures borrowed from computer vision: SegNet for image segmentation together with Bayesian SegNet for uncertainty measurement. We train the network on 3D synthetic volumes and then apply it to field data. We test the proposed approach on a 3D field data set from the Browse Basin, offshore Australia, and a 3D Parihaka seismic data in New Zealand. Applying the weights estimated from training on 3D synthetic volumes to a 3D field data set accurately identifies channel geobodies without the need for any human interpretation on seismic attributes. Our proposed method also produces uncertainty volumes to quantify the trustworthiness of the detection model.

Introduction

Channels are important geologic features for hydrocarbon exploration. However, manual interpretation of channels in seismic images is a time-consuming and subjective process. Numerous methods, such as using coherence attributes, sweetness attributes, and the steerable pyramid, have been proposed for help with channel detection in seismic (Hart, 2008; Mathewson and Hale, 2008; Wu, 2017).

Seismic coherence and other edge-detection algorithms, such as the Sobel filter, can be used to highlight channel boundaries (Kington, 2015; Phillips and Fomel, 2017; Wu, 2017). The directional structure-tensor-based coherence method computes the seismic coherence attribute using eigenvalues of the directional structure-tensors constructed from directional derivatives perpendicular and parallel to the seismic structures (Wu, 2017). These edge-sensitive methods can detect channel edges easily but do not indicate the channel thickness (Liu and Marfurt, 2007). Sweetness is another seismic attribute for channel detection, and it is defined as the ratio between the reflection strength and the square root of the instantaneous frequency (Hart, 2008). Sand-channel bodies generally create stronger, broader reflections than the surrounding shale. Mathewson and Hale (2008) propose steerable pyramid filters to enhance the channel features by partitioning the seismic image with respect to scale and orientation.

All of these seismic attributes focus on detecting the channel boundaries but not the geobodies. We propose to adopt an encoder-decoder convolutional neural

network (CNN) to directly detect 3D channel geobodies without human interpretation on precomputed seismic attributes. The encoder-decoder neural network automatically learns useful features for channel detection. We propose to train the network using a 3D labeled synthetic data set and then use trained parameters to predict channel bodies in 3D seismic field data sets.

Although conventional methods for automatic channel picking lack uncertainty analysis, our proposed method can also provide a quantitative uncertainty analysis. Bayesian SegNet samples the posterior distribution of class probabilities at the test time using drop-out layers (Kendall et al., 2015). The network estimates the mean and variance of the distribution, which can be used to model the uncertainty and provide information to evaluate the risk of decision-making based on interpretation.

Encoder-decoder architecture

CNNs are a specialization of neural networks for data in the form of multiple arrays (LeCun et al., 2015). CNNs replace matrix multiplication in traditional neural networks with a convolution operator to focus on locality and spatial relationship. CNNs can learn highly complex nonlinear relationships in input data with the use of nonlinear activation functions.

Image segmentation in computer vision understands an image at the pixel level, and it assigns each pixel to an object class. Various methods using CNNs have been used for semantic pixel-wise labeling, but the output images are coarse because max-pooling and subsampling

¹The University of Texas at Austin, Bureau of Economic Geology, John A. and Katherine G. Jackson School of Geosciences, University Station, Box X, Austin, Texas 78713-8924, USA. E-mail: nam-pham@utexas.edu (corresponding author); sergey.fomel@beg.utexas.edu; dallas.dunlap@beg.utexas.edu.

Manuscript received by the Editor 31 October 2018; revised manuscript received 29 January 2019; published ahead of production 19 March 2019; published online 22 April 2019. This paper appears in *Interpretation*, Vol. 7, No. 3 (August 2019); p. SE43–SE50, 16 FIGS.

<http://dx.doi.org/10.1190/INT-2018-0202.1>. © 2019 Society of Exploration Geophysicists and American Association of Petroleum Geologists. All rights reserved.

reduce the feature map size (Badrinarayanan et al., 2015). SegNet architecture has encoder layers to learn low-resolution features and uses decoder layers to map them to input resolution for pixel-wise classification (Badrinarayanan et al., 2015) (Figure 1). We define the channel detection problem as an image segmentation task in which we assign a label of channel or non-channel to each pixel of the seismic image. The proposed architecture for automatic channel detection consists of four layers in the encoder and a corresponding four layers in the decoder.

Each encoder layer has a convolutional layer that learns useful features (Figure 2) and a pooling layer. Our architecture for automatic channel detection has 16 trainable filters in each convolutional layer with a size of $3 \times 3 \times 3$. Each filter is only connected to local patches in the feature maps of the previous layer (Le-Cun et al., 2015). Each convolutional layer comes with a batch normalization layer to normalize the data and control overfitting (Ioffe and Szegedy, 2015). The nonlinear activation function ReLU is inserted after the batch normalization layer to learn nonlinear relationships. Max-pooling layers with $2 \times 2 \times 2$ kernels are added in between each convolutional layer to reduce

the spatial size of the feature maps and control overfitting.

Each decoder layer upsamples the input feature maps and convolves the outputs with trainable decoder filters to produce dense maps. Upsampling layers use the transposed convolution algorithm (Dumoulin and Visin, 2016) with learnable $2 \times 2 \times 2$ filters (Figure 3). The coarse outputs are convolved with learnable $3 \times 3 \times 3$ filters to produce denser feature maps (Figure 4). The output from the last decoder layer is fed into a $1 \times 1 \times 1$ convolutional layer to produce feature maps corresponding to two labels of channel or nonchannel. The last layer is the softmax layer that produces the probabilities of each label for each pixel in the seismic image.

Neural networks can be expressed in a Bayesian way to understand the uncertainty (Ghahramani, 2015). The training phase is the transformation of the prior probability distributions $P(\theta|m)$, defined before observing data, into the posterior distributions $P(\theta|D, m)$, defined after observing data:

$$P(\theta|D, m) = \frac{P(D|\theta, m)P(\theta|m)}{P(D|m)}, \quad (1)$$

where D is the observed data, m is the model, and θ is the network parameters. The prediction can also be expressed by the Bayes rule:

$$P(x|D, m) = \int P(x|\theta, D, m)P(\theta|D, m)d\theta, \quad (2)$$

where x is the new data. Different models can be compared by using the Bayes rule:

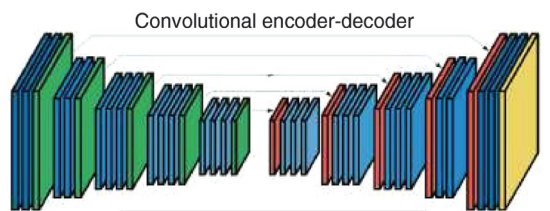


Figure 1. SegNet architecture (image modified after Badrinarayanan et al., 2015).

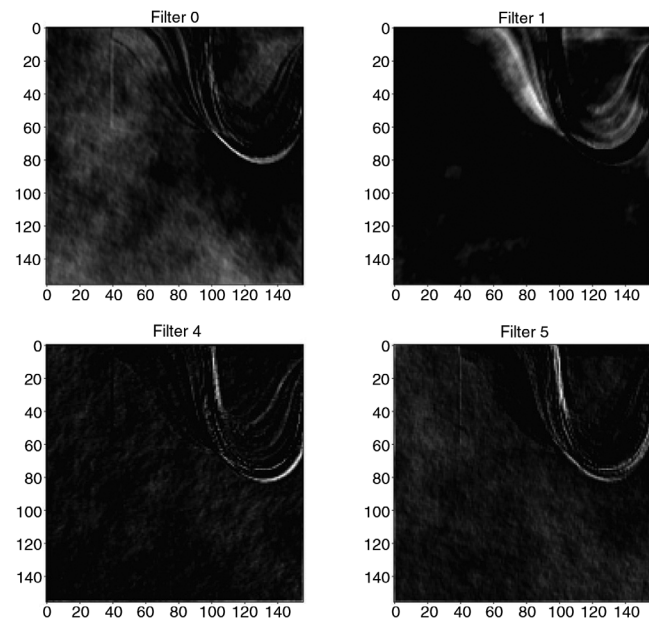
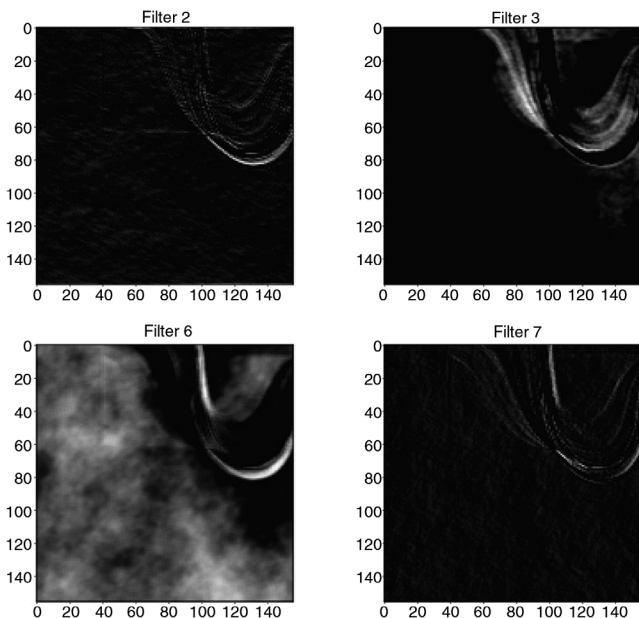


Figure 2. Eight example feature maps generated by a convolutional layer.



$$P(m|D) = \frac{P(D|m)P(m)}{P(D)}. \quad (3)$$

The uncertainty of neural networks can come from many sources such as parameter uncertainty and model structure uncertainty. Bayesian SegNet is a development of SegNet architecture and a probabilistic image segmentation framework understanding the network parameters uncertainty by using dropout layers (Kendall et al., 2015). The dropout method randomly removes units in a network, which is a way of getting samples from the posterior distribution of softmax class

probabilities. Therefore, dropout is an approximation of the Bayesian inference over the network's weights (Gal and Ghahramani, 2015b). It can be used at test time to create a Bernoulli distribution over the filter's weights (Gal and Ghahramani, 2015a). Our model has a dropout layer between the last encoder layer and the first decoder layer, which removes 30% of the units. An Adam optimizer (Kingma and Ba, 2014) with 0.1 as the learning rate is used for backpropagation. We take 30 samples at test time and calculate the variance of the distribution over the probabilities of the channel to quantify the prediction uncertainty.

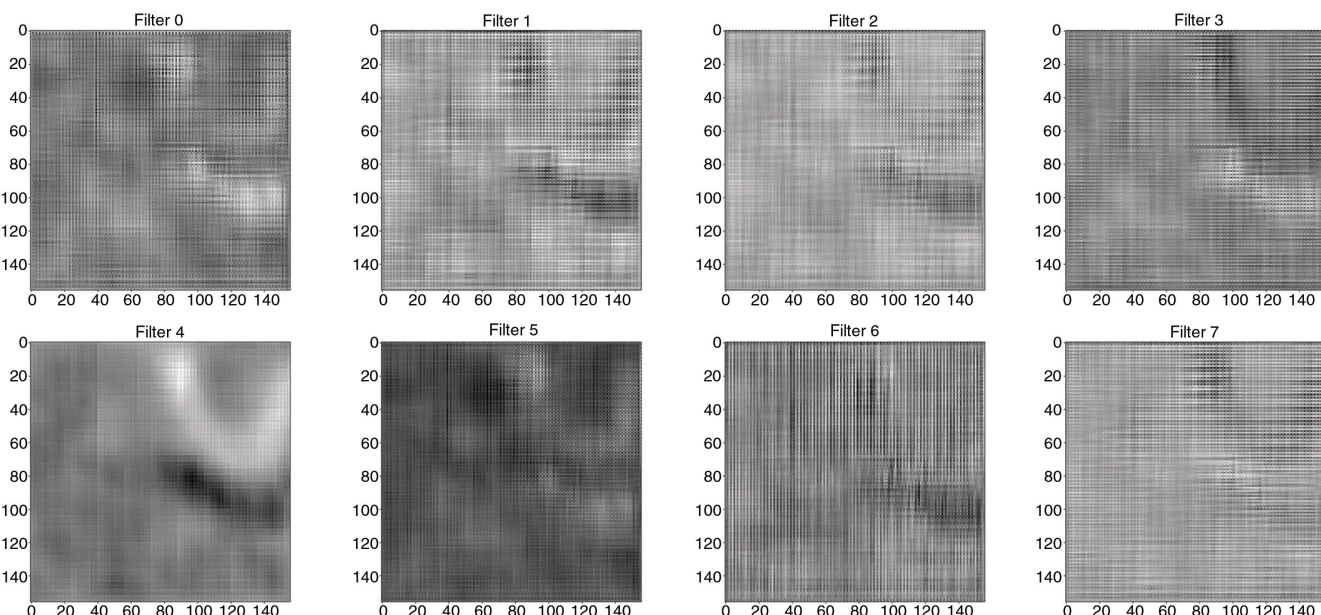


Figure 3. Eight example feature maps generated by the transposed convolution upsample filters.

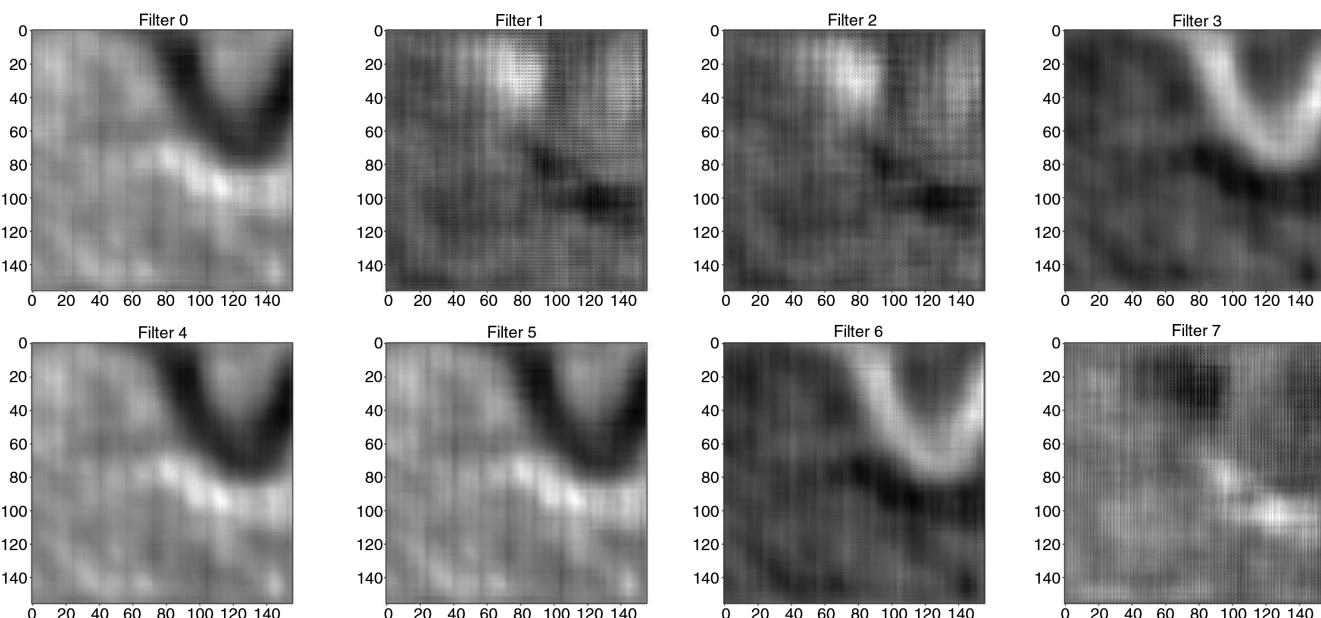


Figure 4. Eight example feature maps generated by the denser upsample filters.

Training

Training data

For the training data, we choose a 3D convolutional synthetic depth model created by James Jennings at the Bureau of Economic Geology, Austin, Texas, in collaboration with Chevron (Figure 5a). The data simulate a

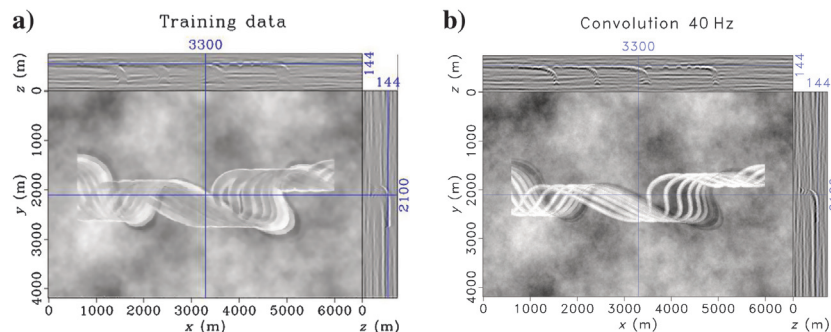


Figure 5. (a) Synthetic training data. (b) An example of synthetic training data with thin channels.

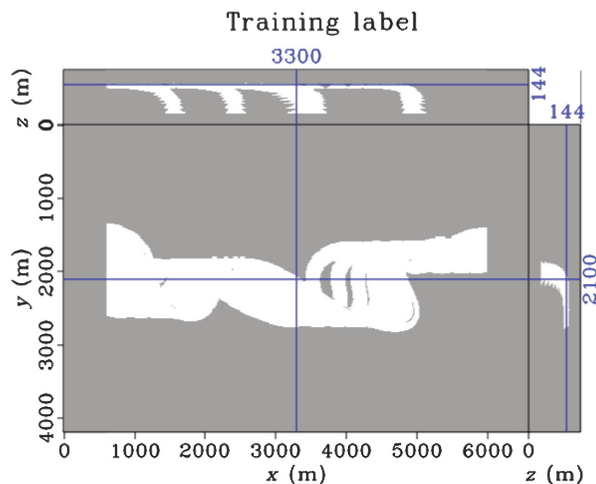


Figure 6. Training label.

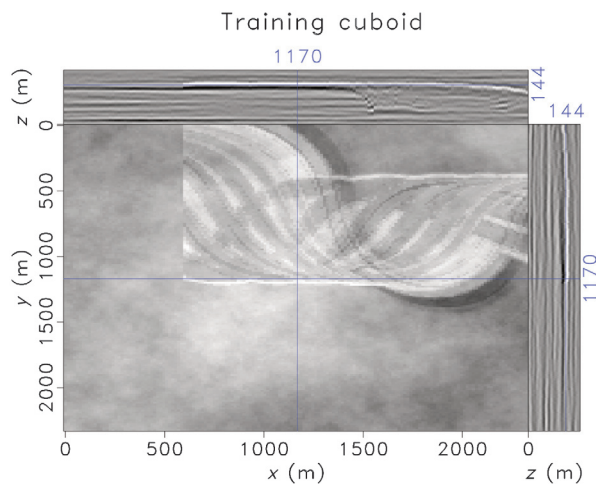


Figure 7. Training cuboid.

complex deepwater stacked channel system in Africa with correlated noise in porosity. On top of the channel is an overburden with stochastically generated velocity fluctuations and correlated noise in porosity (Fomel et al., 2007). The dominant frequency of the seismic wavelet is 40 Hz. The data are created by three pieces of information: 3D shallow high-resolution seismic data are used together with an analytical curve to simulate the shape of the channels, a group of geologists study the channel properties distribution at an analog outcrop in California, and the background information is created by geostatistics.

We eliminate the noise in the channel bodies and subtract the result from original data to obtain the location of channels. We create the labels by masking the channel location with one and everywhere else with zero (Figure 6). We modify different channel properties, such as the amalgamated sand cross-section shape parameter, porosity, dominant frequency, and channel thickness to create a diverse training data set (Figure 5b). Because of limited computational resources, a training batch has four seismic volumes with a size of $156 \times 156 \times 100$ samples (Figure 7). Examples in the training data overlap one another, but that is a way of augmenting the data. We generate a total of 1025 training examples with six examples for validating the network.

Training result

We trained our network on the synthetic data for 33 epochs in 4 h using a Titan Xp GPU. The mean value of the intersection over the union (Mean IU) is the accuracy metric defined as

$$\left(\frac{1}{n_{cl}} \right) \sum_i \frac{n_{ii}}{\sum_j n_{ij} + \sum_j n_{ji} - n_{ii}}, \quad (4)$$

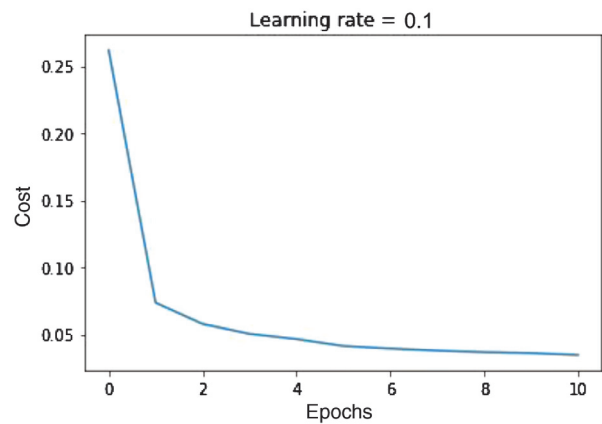


Figure 8. Training cost in 10 epochs.

where n_{cl} is the number of classes and n_{ij} is the number of pixels of class i predicted to belong to class j (Long et al., 2014). The cross-entropy cost decreases during training (Figure 8), and the mean IU is 93.5% after training. The global accuracy defined as the percentage of pixels correctly classified in the image increases during training and reaches 99%. Applying the trained model to six unseen validation examples, we obtain the mean IU of 93%, which is close to the training mean IU. Comparing with the true label of a vertical slice in Figure 9b, channel bodies are picked clearly in the synthetic data set (Figure 9c).

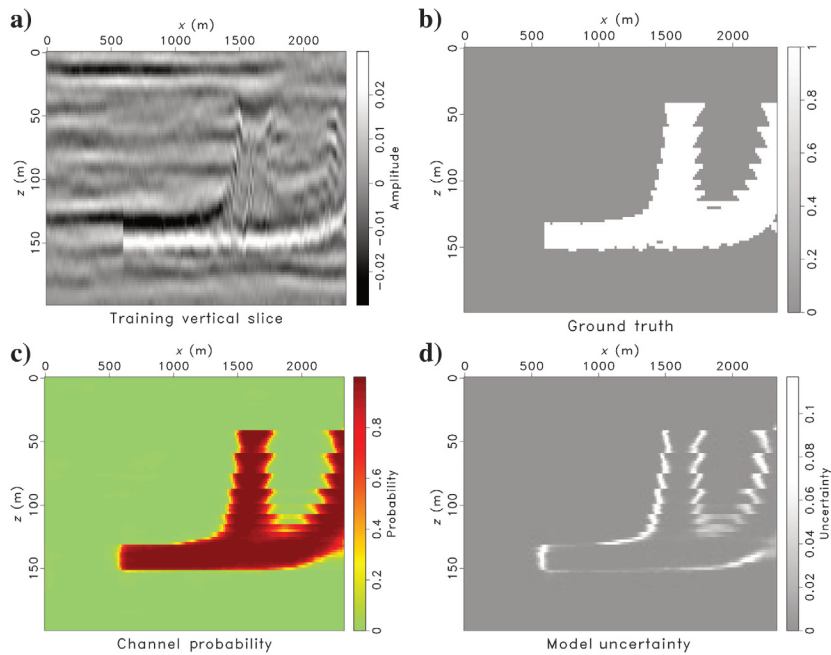


Figure 9. (a) Training vertical slice. (b) Ground truth of the training vertical slice. (c) Channel probability in the vertical slice. (d) Model uncertainty in the vertical slice.

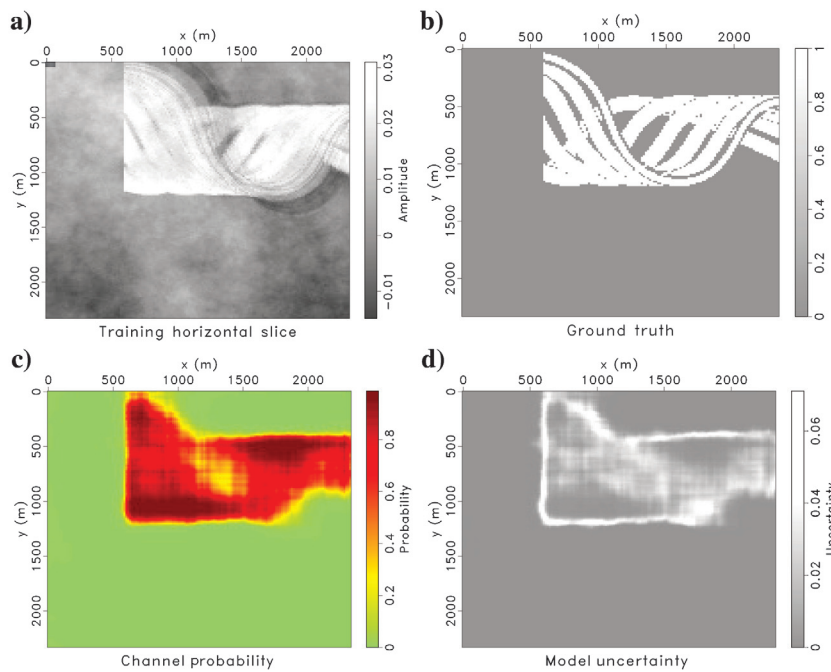


Figure 10. (a) Training horizontal slice. (b) Ground truth of the training horizontal slice. (c) Channel probability in the horizontal slice. (d) Model uncertainty in the horizontal slice.

The model uncertainty from Bayesian SegNet can be used to understand how confidently we can trust the channel segmentation. At boundaries of the channels, the prediction has high uncertainty (Figure 9d), which reflects the ambiguity of the network surrounding the definition of defining the transition between the channel and nonchannel areas (Kendall et al., 2015). Compared with true label of a horizontal slice in Figure 10b, the model can successfully pick the channel geobodies (Figure 10c). However, it is difficult to distinguish individual channels in the data set, so there is high uncertainty when there are multiple channels (Figure 10d).

Testing

Browse basin data set

We apply the weights from training the synthetic data to a $312 \times 312 \times 100$ subvolume of a field data set from offshore Australia (Figure 11). The data set is a 3D marine seismic survey located in 2500 m of water depth with a sample rate of 2 ms and a dominant frequency of 120 Hz. The data set is in depth with a sampling interval of 2 m. The seismic data host numerous stacked deep-water channel-levee complexes. We divide the subvolume into 16 small overlapping volumes of size $156 \times 156 \times 100$ samples using the nonstationary patching method (Claerbout, 2014) to eliminate the edge artifacts and test each volume independently. The testing output volumes are stitched together using the inverse of the nonstationary patching method with weighted boundaries. Figure 12a shows that the channel bodies are clearly picked in the seismic volume. We analyze the prediction uncertainty by using the variance of 30 samples from the posterior distribution of channel probability (Figure 13).

When there are multiple channels in the data set (the black circle in Figure 11), the trained model cannot distinguish individual channels very well and the

prediction uncertainty is high. The trained model can detect thin channels in the data set with not too high probabilities, but the uncertainty map displays high values in these regions (the red circles in Figure 11). Therefore, the prediction uncertainty has useful information for the channels detection task and interpreters can repick the regions with high uncertainty to enhance the detection result from neural network. Our result follows the channel edges enhanced by plane-wave destruction Sobel filter (Phillips and Fomel, 2017) (Figure 12b), with the addition of model uncertainty.

Parihaka data set

We apply the weights from training the synthetic data to a $501 \times 750 \times 251$ subvolume of the Parihaka data set in New Zealand (Figure 14). The relative coarse-grained channel deposits are at the base of the incisional channel systems, which is different from the Australian data set where the coarse-grained channel deposits are vertically stacked. The data set is in time with a sample rate of 4 ms. We also use the nonstationary patching method (Claerbout, 2014) to divide the subvolume into small overlapping volumes of size $156 \times 156 \times 100$ samples to eliminate edge artifacts. The trained neural network model successfully picks the channel bodies in the seismic volume with high probabilities (Figure 15a). The model uncertainty is calculated by using the variance of 30 samples from the posterior distribution of the channel probability (Figure 16). The Parihaka data set is different from our synthetic training data set, so when applying our trained model, it is hard to produce a clean probability volume. However, high channel probabilities follow the channel edges enhanced by plane-wave destruction Sobel filter (Phillips and Fomel, 2017) (Figure 15b) with the addition of model uncertainty.

Conclusion

We propose a method for automatic detection of channel bodies in seismic images using an encoder-decoder CNN. The network is trained on synthetic training data and is then applied to field data.

We test the model on field data sets from offshore Australia and New Zealand. With only training on the synthetic data set, the model successfully identifies

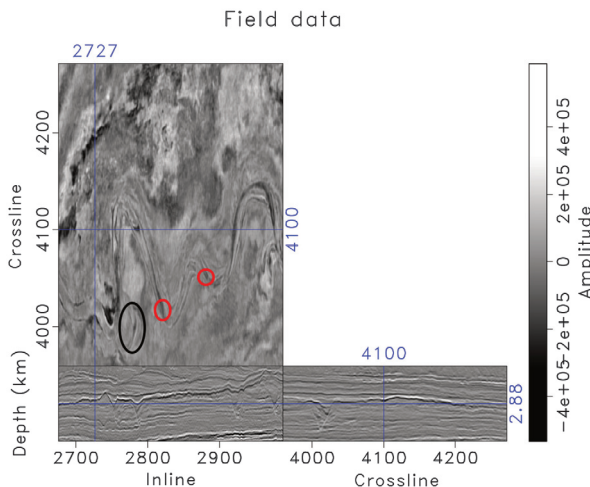
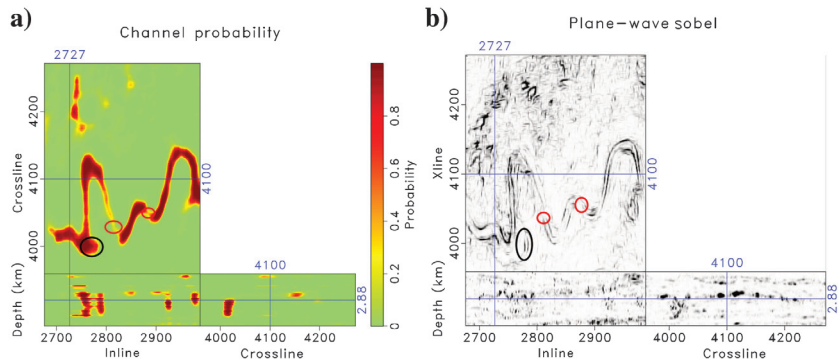


Figure 11. Australia field data set (the red circles are thin channel areas, and the black circles are multiple channel areas).

Figure 12. (a) Channel probability in the Australia field data set. (b) Channel boundaries enhancement in the Australia data set by PWD Sobel filter (the red circles are thin channel areas, and the black circles are multiple channels areas).



the channel bodies in the field data sets. The prediction uncertainty is computed simultaneously and can help an interpreter judge and enhance the channel detection results.

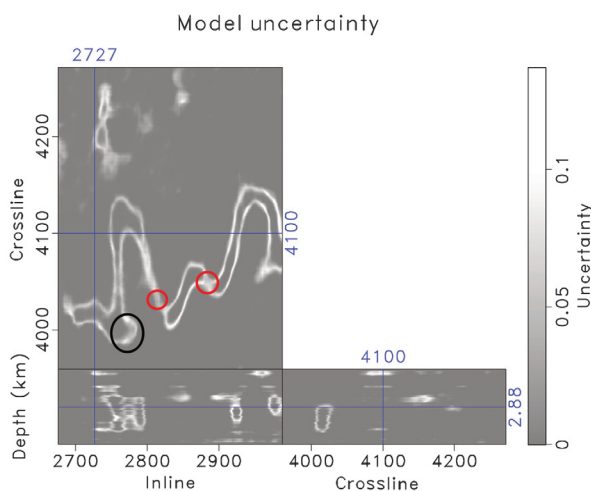


Figure 13. Model uncertainty in the Australia field data set (the red circles are thin channel areas, and the black circles are multiple channels areas).

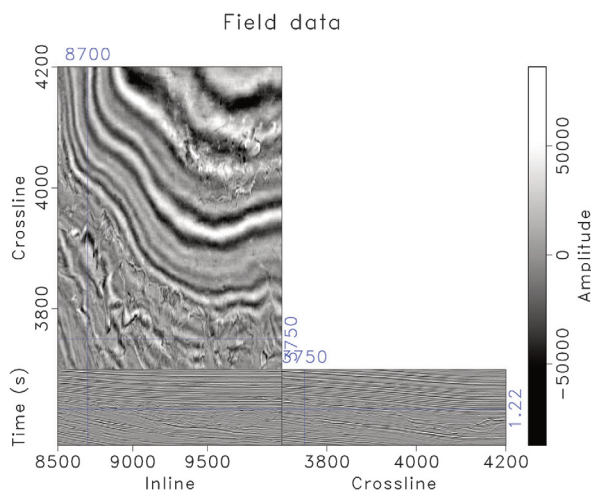


Figure 14. Parihaka field data set.

We believe that the proposed method has great future potential for automatic interpretation and quantitative analysis. Neural network models are trained with synthetic data sets created by the knowledge of experts from geologists, geophysicists, and petroleum engineers, and then the trained models are applied to field data sets to perform interpretation tasks such as faults, salt, and channel geobodies detection. Our results can be improved using more diverse labeled training data sets. Future research will also combine object detection and semantic segmentation to clearly image individual channels.

Acknowledgments

We thank the sponsors of the Texas Consortium for Computational Seismology for their financial support. We also thank the NVIDIA GPU Grant Program for providing the Titan Xp. The field data sets are provided by J. Covault from the Quantitative Clastics Laboratory. The synthetic data set was simulated by J. Jennings in collaboration with Chevron. We also acknowledge the donation of the Landmark graphics interpretation software through the Landmark Graphics University Grant Program and GeoScience Australia for data

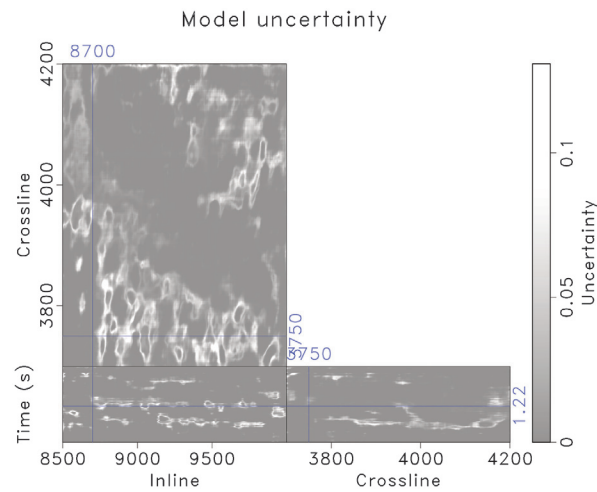


Figure 16. Model uncertainty in the Parihaka field data set.

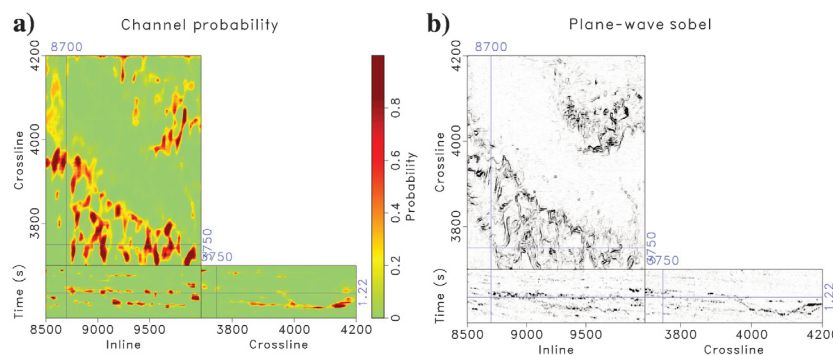


Figure 15. (a) Channel probability in the Parihaka field data set. (b) Channel boundary enhancement in the Parihaka data set by the PWD Sobel filter.

access. We thank Y. Shi and X. Wu for their helpful discussions.

Data and materials availability

Data associated with this research are available and can be obtained by contacting the corresponding author.

References

- Badrinarayanan, V., A. Kendall, and R. Cipolla, 2015, Segnet: A deep convolutional encoder-decoder architecture for image segmentation: CoRR, abs/1511.00561.
- Claerbout, J., 2014, Geophysical image estimation by example: Lulu.com.
- Dumoulin, V., and F. Visin, 2016, A guide to convolution arithmetic for deep learning: CoRR, abs/1603.07285.
- Fomel, S., E. Landa, and M. T. Taner, 2007, Poststack velocity analysis by separation and imaging of seismic diffractions: *Geophysics*, **72**, no. 6, U89–U94, doi: [10.1190/1.2781533](https://doi.org/10.1190/1.2781533).
- Gal, Y., and Z. Ghahramani, 2015a, Bayesian convolutional neural networks with Bernoulli approximate variational inference: CoRR, abs/1506.02158.
- Gal, Y., and Z. Ghahramani, 2015b, Dropout as a Bayesian approximation: Representing model uncertainty in deep learning: ArXiv preprint arXiv:1506.02142.
- Ghahramani, Z., 2015, Probabilistic machine learning and artificial intelligence: *Nature*, **521**, 452–459, doi: [10.1038/nature14541](https://doi.org/10.1038/nature14541).
- Hart, B. S., 2008, Channel detection in 3-D seismic data using sweetness: *AAPG Bulletin*, **92**, 733–742, doi: [10.1306/02050807127](https://doi.org/10.1306/02050807127).
- Ioffe, S., and C. Szegedy, 2015, Batch normalization: Accelerating deep network training by reducing internal covariate shift: CoRR, abs/1502.03167.
- Kendall, A., V. Badrinarayanan, and R. Cipolla, 2015, Bayesian segnet: Model uncertainty in deep convolutional encoder-decoder architectures for scene understanding: CoRR, abs/1511.02680.
- Kingma, D. P., and J. Ba, 2014, Adam: A method for stochastic optimization: CoRR, abs/1412.6980.
- Kington, J., 2015, Semblance, coherence, and other discontinuity attributes: *The Leading Edge*, **34**, 1510–1512, doi: [10.1190/tle34121510.1](https://doi.org/10.1190/tle34121510.1).
- LeCun, Y., Y. Bengio, and G. E. Hinton, 2015, Deep learning: *Nature*, **521**, 436–444, doi: [10.1038/nature14539](https://doi.org/10.1038/nature14539).
- Liu, J., and K. J. Marfurt, 2007, Instantaneous spectral attributes to detect channels: *Geophysics*, **72**, no. 2, P23–P31, doi: [10.1190/1.2428268](https://doi.org/10.1190/1.2428268).
- Long, J., E. Shelhamer, and T. Darrell, 2014, Fully convolutional networks for semantic segmentation: CoRR, abs/1411.4038.
- Mathewson, J., and D. Hale, 2008, Detection of channels in seismic images using the steerable pyramid: Colorado School of Mines.
- Phillips, M., and S. Fomel, 2017, Plane-wave sobel attribute for discontinuity enhancement in seismic images: *Geophysics*, **82**, no. 6, WB63–WB69, doi: [10.1190/geo2017-0233.1](https://doi.org/10.1190/geo2017-0233.1).
- Wu, X., 2017, Directional structure-tensor-based coherence to detect seismic faults and channels: *Geophysics*, **82**, no. 2, A13–A17, doi: [10.1190/geo2016-0473.1](https://doi.org/10.1190/geo2016-0473.1).

Biographies and photographs of the authors are not available.